Evolution of density-dependent movement during replicated experimental range expansions

Emanuel A. Fronhofer[1,2,*], Sereina Gut[1] and Florian Altermatt[1,2]

1 Eawag: Swiss Federal Institute of Aquatic Science and Technology, Department of Aquatic Ecology, Überlandstrasse 133, CH-8600 Dübendorf, Switzerland

2 Department of Evolutionary Biology and Environmental Studies, University of Zurich, Winterthurerstrasse 190, CH-8057 Zürich, Switzerland

* Orcid ID: 0000-0002-2219-784X

Running title: Evolution during range expansions

Keywords: Dispersal evolution, context-dependent dispersal, experimental evolution, protist microcosm, biological invasion, *Tetrahymena thermophila*

Correspondence Details
Emanuel A. Fronhofer
Eawag: Swiss Federal Institute of Aquatic Science and Technology
Department of Aquatic Ecology
Überlandstrasse 133
CH-8600 Dübendorf
phone: +41 58 765 5143
email: emanuel.fronhofer@eawag.ch

Abstract

Range expansions and biological invasions are prime examples of non-equilibrium systems that are likely impacted by rapid evolutionary changes. As a spatial process, range expansions are driven by dispersal and movement behaviour. While it is widely accepted that dispersal and movement may be context-dependent, for instance density-dependent, and best represented by reaction norms, the evolution of density-dependent movement during range expansions has received very little experimental attention. We therefore tested current theory predicting the evolution of density-independent movement at range margins using highly replicated and controlled range expansion experiments with 14 genotypes of the protist model system *Tetrahymena thermophila*. Although rare, we found evolutionary changes during range expansions even in the absence of initial standing genetic variation. Range expansions led to the de novo evolution for completely density-independent movement at range margins and a positive density-dependent movement reaction norm in range cores. In addition, we report the evolution of increased reproductive rates at range margins and slightly increased competitive ability in range cores. Our findings highlight the importance of understanding dispersal as an evolving reaction norm and a plastic life-history trait of central relevance for range expansions, biological invasions and the dynamics of spatially structured systems in general.

Introduction

Species' ranges and the distribution of taxa on earth have long been studied only from an ecological point of view and put in the context of local climatic and environmental conditions. Recent theoretical work and empirical case examples, however, indicate that this approach suffers from some shortcomings. Most importantly, this perspective is static in the sense that evolutionary changes are usually ignored. However, rapid evolutionary changes are thought to be especially relevant under transient and non-equilibrium conditions inherent to species range dynamics and population spread (Excoffier et al., 2009; Hanski, 2012; Kubisch et al., 2014).

The importance of an evolutionary and eco-evolutionary perspective to understanding the dynamics of species ranges becomes evident when considering the main drivers of range dynamics: dispersal and reproduction. Both of these life-history traits likely have a genetic basis (Bonte and Dahirel, 2017) and can thus be subject to evolutionary change. Ample theoretical evidence suggests that the evolution of dispersal and reproduction may have important effects on the dynamics of species ranges (e.g. reviewed in Kubisch et al., 2014). For instance, dispersal during range expansions is predicted to evolve to higher rates at range margins, a phenomenon which has been called 'spatial selection' (Phillips et al., 2010). Spatial selection relies on a simple ecological filter effect: if there is variation in dispersal ability, fast individuals will automatically be spreading more towards the range margin and colonize previously empty patches (see also Haag et al., 2005). As a consequence, populations at the range margin have a high proportion of highly dispersive individuals that will mate with each other. In combination with fitness advantages due to low intraspecific competition at the range margin, this spatial assortment can lead to the evolution of increased dispersal and movement abilities. These evolutionary changes have important consequences for (macro)ecological patterns: range expansions and biological invasions are predicted to proceed faster if dispersal evolves (Perkins et al., 2013). Theoretical predictions regarding the evolution of reproduction have also been made, especially in the context of life-history trade-offs between dispersal, reproduction and competitive ability (Burton et al., 2010; Fronhofer and Altermatt, 2015; Fronhofer et al., in press). Since dispersal is costly (Bonte et al., 2012), models generally assume that either reproduction or competitive ability have to decrease if dispersal increases.

While there is accumulating comparative empirical evidence linked to spatial selection (e.g. Thomas et al., 2001; Phillips et al., 2006; Lombaert et al., 2014), experimental confirmation is more scare. This scarcity is mainly due to the obvious challenges associated with studying how evolution impacts macroecological patterns experimentally. However, a recently increasing use of (small) model organisms has been spurring the study of experimental range expansions and population spread dynamics. As a consequence, range expansions are currently under intense scrutiny from an experimental ecological (Melbourne and

Hastings, 2009; Giometto et al., 2014) and evolutionary point of view (Fronhofer and Altermatt, 2015; Williams et al., 2016; Wagner et al., 2016; Ochocki and Miller, 2017; Weiss-Lehman et al., 2017; Fronhofer et al., in press). A result of these concerted efforts is the experimental demonstration that range expansions indeed may select for increased dispersal rates and distances at the rage margin (in protists: Fronhofer and Altermatt 2015; Fronhofer et al. in press; in insects: Ochocki and Miller 2017; Weiss-Lehman et al. 2017 and in plants: Williams et al. 2016) which can lead to increased range expansion speeds.

All of these studies represent important advances for our understanding of how evolutionary change impacts range expansions. However, these current experimental studies generally considered selection on already existing standing genetic variation. This is a strong assumption, especially in the context of biological invasions, since standing genetic variation is usually depleted due to bottlenecks associated to the invasions process itself, which potentially constrains evolutionary dynamics. Furthermore, these works strongly simplify the dispersal trait and focus on unconditional dispersal (but see, e.g. Fronhofer et al., in press; Weiss-Lehman et al., 2017). This may often be unrealistic, especially as dispersal and movement are well-known to be highly context-dependent (Clobert et al., 2009). Consequently, dispersal properties are much better represented by a reaction norm (Pennekamp et al., 2014; Fronhofer et al., 2015b). The most well-known dispersal reaction norm captures dispersal as a function of conspecific density, as the spatio-temporal distribution of densities is an important proximate and ultimate factor determining dispersal strategies (Bowler and Benton, 2005; Ronce, 2007).

Current theory predicts that range expansions do not only select on the mean dispersal trait, but rather on the shape of the reaction norm (Travis et al., 2009). As a key consequence thereof, dispersal is predicted to become density-independent at the range margin (Travis et al., 2009). While density-dependent dispersal will optimize fitness in (quasi)equilibrium environments, such as the range core (Bowler and Benton, 2005), local conspecific density does not provide relevant information at the range margin: spatial selection makes dispersal highly advantageous even if local densities at the range margin are low. The evolution of density-independent dispersal at the range margin may have important consequences for range expansion dynamics: theory shows that density-dependent dispersal may slow down range expansions (Best et al., 2007) but can ultimately lead to wider ranges (Kubisch et al., 2011), to name but two examples.

Here, we experimentally tested whether and how range expansions impact the evolution of density-dependent movement (as a proxy of dispersal) and potentially change the shape of the density-dependent movement reaction norm. We predicted movement to evolve towards density-independence at the range margin (Travis et al., 2009; Weiss-Lehman et al., 2017). We tested this prediction using experimental evolution and replicated range expansions of 14 clonally reproducing *Tetrahymena thermophila* strains,

as well as the mix of these strains. Due to the lack of initial standing genetic variation in the replicates with single clonal strains and the low population densities characteristic of expanding range margins, we predicted consistent evolutionary differentiation between range core and margin populations to be rare and emerge only in a minority of our replicates. Investigating the consequences of lacking initial standing genetic variation sets our approach apart from previous work on range expansions, makes it more relevant in the context of biological invasions, and also allowed us to focus on newly emerging differentiation in life-history traits along a species' range. In addition to movement behaviour, we also recorded changes in other life-history traits, namely reproduction and competitive ability, to investigate potential concurrent evolutionary changes (Bonte and Dahirel, 2017).

Material and Methods

Model organism

We used the freshwater ciliate *Tetrahymena thermophila* (Cassidy-Hanley, 2012) as our model organism. It is, together with its sister species (*Tetrahymena pyriformis*), commonly and successfully employed in both ecological (e.g., Giometto et al., 2014; Fronhofer et al., 2015b) and evolutionary contexts (e.g., Fjerdingstad et al., 2007; Friman et al., 2011; Pennekamp et al., 2014; Hiltunen and Becks, 2014; Fronhofer and Altermatt, 2015) and is known to show density-dependent movement and dispersal (Pennekamp et al., 2014; Fronhofer et al., 2015b). *Tetrahymena thermophila* can reproduce both sexually (if a cell from another mating type is present) and clonally. We used a total of 14 clonally reproducing strains which were isolated as single cells shortly prior to the experiment from 7 mating types originally obtained from Cornell University's Tetrahymena Stock Center (Stock ID: MTP01). The 14 clonally reproducing strains used here differ in attributes ranging from population growth rates and equilibrium densities (Tab. S1) to morphology and movement characteristics (Tab. S2).

Tetrahymena thermophila was kept in filtered (cellulose paper filters, 4–7 μm; Whatman) and autoclaved protist pellet medium (0.46 gL^{-1}; Protozoan pellets, Carolina Biological Supply) under constant temperature (20°C) and light conditions (Osram Biolux 30W). Initially, we supplemented the medium with a mix of three bacterial species (*Serratia fonticola*, *Bacillus subtilis* and *Brevibacillus brevis*; obtained from Carolina Biological Supply) at approx. 5% of their equilibrium density as a food source. During the experiment we replaced 2 mL out of 15 mL medium in each microcosm with bacterial cultures at equilibrium density (approx. 1 week old) in order to prevent adaptation of the bacteria and co-evolutionary dynamics from occurring. For further methodological details see Altermatt et al. (2015).

Experimental setup and microcosm landscapes

We set up microcosm landscapes to study range expansions into initially uninhabited habitat by propagating range core and range margin populations as described by Fronhofer and Altermatt (2015). The microcosms landscapes consisted of two vials (20mL conical vials, Sarstedt) connect by silicone tubing (inside diameter: 4mm, VWR) and a stopcock (Discofix, B.Braun) to control for dispersal (total length: 6cm).

The first patch (start) was initially filled with the respective *T. thermophila* strain at equilibrium density and dispersal into the empty target patch (filled with 15 mL bacterized protist pellet medium) was allowed for 4 h. The dispersal phase was followed by a 1-day regrowth phase after which the populations in the start and target patches were propagated to start patches in respectively new 2-patch systems. The population from the original start patch was subsequently taken as the range core. Dispersal was allowed for 4 h and only the individuals remaining in the start patch were further propagated. By contrast, the population from the original target patch represented the range margin. Dispersal was also allowed for 4 h. Thereafter, the population in the target patch was propagated to a new 2-patch system. This procedure, effectively tracking range core and expanding range margin populations, was repeated 3 times per week for 1 month.

During transfer to new 2-patch systems only 13 of the 15 mL of the range core were transferred and the remaining 2 mL were filled with bacterial cultures at equilibrium (approx. 1 week old) to avoid evolutionary changes in the bacterial populations. This procedure was not necessary for the range margin, as the individuals of the range margin had always just dispersed into freshly bacterized medium.

We chose this experimental approach that tracks only range core and range margin for convenience and feasibility. Firstly, we can easily control resource levels and avoid loss of control and contaminations due to aging medium in long landscapes. Secondly, we have shown that, although the experimental procedure obviously prevents feedbacks between core and margin populations, our results are not altered if we indeed use long interconnected linear landscapes (Fronhofer et al., in press).

We followed a total of 48 range expansions, that is, pairs of range cores and margins. We replicated the range expansion of each of the 14 strain three times and additionally included six replicates of a mix (in equal proportions) of all strains. The latter range expansions using the mix of strains thus differs from the range expansions of the single clones in that they were started with standing genetic variation and that sexual reproduction could occur due to the presence of multiple mating types.

Recording of population densities and movement data

During the experiment all microcosms were sampled at every transfer, that is three times per week. Data on population densities as well as movement metrics (e.g., velocity of the cells) were collected by video recording and automated analysis.

Using a Leica M205C stereomicroscope at a 16-fold magnification and an Orca Flash 4 camera (Hamamatsu) we recorded 20 s videos (25 frames per second) of an effective volume of 34.4 μL (sample height: 0.5 mm). Videos were subsequently analysed using the R environment for statistical computing (version 3.2.3) and a customized version of the 'BEMOVI' package (available on GitHub: https://github.com/efronhofer/bemovi) originally developed by Pennekamp et al. (2015). The 'BEMOVI' package uses the image processing software ImageJ to locate moving particles in the videos and to calculate population densities as well as movement metrics. Data are automatically filtered to exclude artifacts such as debris that are outside the size or movement range of the study species (detailed settings available on GitHub: https://github.com/efronhofer/analysis_script_bemovi). As movement velocity has been shown to correlate well with dispersal rates in this system (Fronhofer and Altermatt, 2015; Fronhofer et al., 2015a) we will focus on velocity as a proxy for dispersal.

Common garden experiments

In order to separate evolutionary from potential environmental effects, movement behaviour of individuals from range core and range margin populations was measured not only during the evolution experiment, but also after the end of the experiment and a three-day common garden phase (doubling time for the strains of *T. thermophila* used here: approx. 3–12 h; see Tab. S1). The common garden was initiated with 1.5 mL samples obtained from the respective core and margin populations from the last day of the evolution experiment that were added to 13.5 mL freshly bacterized medium to homogenize environmental conditions.

In addition, we kept a subset of the individuals analysed in this first common garden for an extended period in a common environment (total of 38 days). This allowed us to explore the long-term stability of potential evolutionary changes. Resources were not refreshed in order to create strong competition similar to stable range core populations.

Estimating population growth rates and competition coefficients

Both, at the beginning of the experiment and after the common garden we used growth curve experiments to assess population growth and estimate population growth rates (r_0) as well as competition coefficients (α_{ii}). These experiments were always started with 1 mL of the respective strain (1 week old for the

beginning; from the common garden for the end) and 14 mL freshly bacterized medium. We then followed population densities and movement over the course of 9 days, measuring twice in the first two days and then once on days 2, 3, 4, 7 and 9.

Population growth rates (r_0) and competition coefficients (α_{ii}) were estimated by fitting the logistic growth model according to Verhulst (1838)

$$\frac{dN}{dt} = (r_0 - \alpha_{ii}N)N \tag{1}$$

where N is the population size, to the data obtained from the growth experiments. The equilibrium density is obtained as $\hat{N} = \frac{r_0}{\alpha_{ii}}$. We used the R environment for statistical computing (version 3.3.2) to solve (function 'ode'; 'deSolve' package) and subsequently fit the model by minimizing residuals using the Levenberg-Marquardt algorithm (function 'nls.lm'; 'minpack.lm').

Density-dependent movement

The data obtained from the growth experiments were also used to assess potential evolutionary changes in density-dependent movement, that is, velocity as a function of relative population density ($\frac{N}{\hat{N}}$). Correlating population densities and movement may be challenging: for instance, low densities due to declining or growing populations may lead to very different movement decisions, as protists likely base movement decisions on chemical cues (Fronhofer et al., 2015b). We therefore determined whether there was an indication for a decay phase towards the end of the growth experiments by additionally fitting a logistic model that allows for decaying population densities. This growth model follows Eq. 1, however it assumes that $\alpha_{ii} = \alpha_0(1 + \beta(t - t_{crit}))$ if $t > t_{crit}$ where α_0 is a baseline competitive ability, β the rate at which competition increases over time (t) and t_{crit} the critical time point from which on the increase in competition (respectively decrease in equilibrium density) occurs. Although we did not find an indication for the presence of a clear decay (mean Akaike Information Criterion corrected for sampling size, AICc, over all fits for the logistic: 152.1; mean AICc over all fits for the decay-logistic: 166.3) we decided to be conservative in our analysis and excluded all movement data of day 7 of the growth experiment onwards as both mean and median values of t_{crit} estimates were approx. 7 days.

Statistical analyses

All data were analysed statistically using the R environment for statistical computing (version 3.3.2) and linear mixed models (function 'lme'; 'nlme' package). Response variables were appropriately transformed (see Supporting Information Tab. S3 – S7) to satisfy model assumptions.

More specifically, movement velocity was analysed using individual based velocity data with 'time'

nested in 'replicate' as a random effect structure to account for the non-independence of individuals measured in one sample as well as the temporal non-independence of the repeated measures through time. All models, from the null model to the model including an interaction between the two explanatory variables 'time' and 'range border position' were implemented. We used model selection based on AICc and maximum likelihood (ML) estimates obtained with the 'optim' optimizer. Subsequently, the best fitting model was refit using REML to obtain model estimates.

Density-dependent movement was analysed in analogy to movement as described above with the difference that 'population density' and 'population history' (range border position and starting populations) were interacting fixed effects. The analysis of population growth rates (r_0) and competition coefficients (α_{ii}) followed the same logic, however model selection only included the null model and the model with population history (range border position and starting populations) as a fixed effect as well as 'strain ID' as a random effect. The random effect structure was chosen, as growth rates and competition coefficients of all successfully expanding strains, regardless of their evolutionary difference in dispersal, were used in this analysis. We followed this approach in order to obtain a sufficient sample size since growth rates and competition coefficients are population level measures.

Finally, differences between failed and successful range expansions, that is, experimental replicates in which the range margin failed to expand and went extinct versus those that kept up with our experimental treatment, were analysed by correlating growth rates (r_0), competition coefficients (α_{ii}) as well as median and standard deviation of movement velocity of the starting populations with invasion success (yes/ no). As a random effect we included 'strain ID' in order to account for the non-independence of replicates. Model selection was performed as described above.

AICc values, AICc weights and sample sizes can be found in the Supporting Information Tab. S3 – S7. In the main text we only describe the best fitting model and visualize model estimates and the corresponding confidence intervals. The data are available at Dryad (http://dx.doi.org/xxxxx).

Results

Range expansion success

As predicted, successful range expansions were rare: out of 48 replicated range expansions only 4 replicates belonging to three clonal strains (Fig. 1 C, H and K; Tab. S3) successfully tracked our experimental treatment and expanded their range over the entire duration of the experiment. All other replicates of both clonal strains and the genetically mixed population (Fig. 1 O) only tracked the range expansion over part of the experimental duration and subsequently went extinct at the range margin. The three successfully expanding strains (Fig. 1 C, H and K) did, at the start of the experiment, not statistically

differ from all other stains based on their initial properties (Fig. S1; Tab. S7).

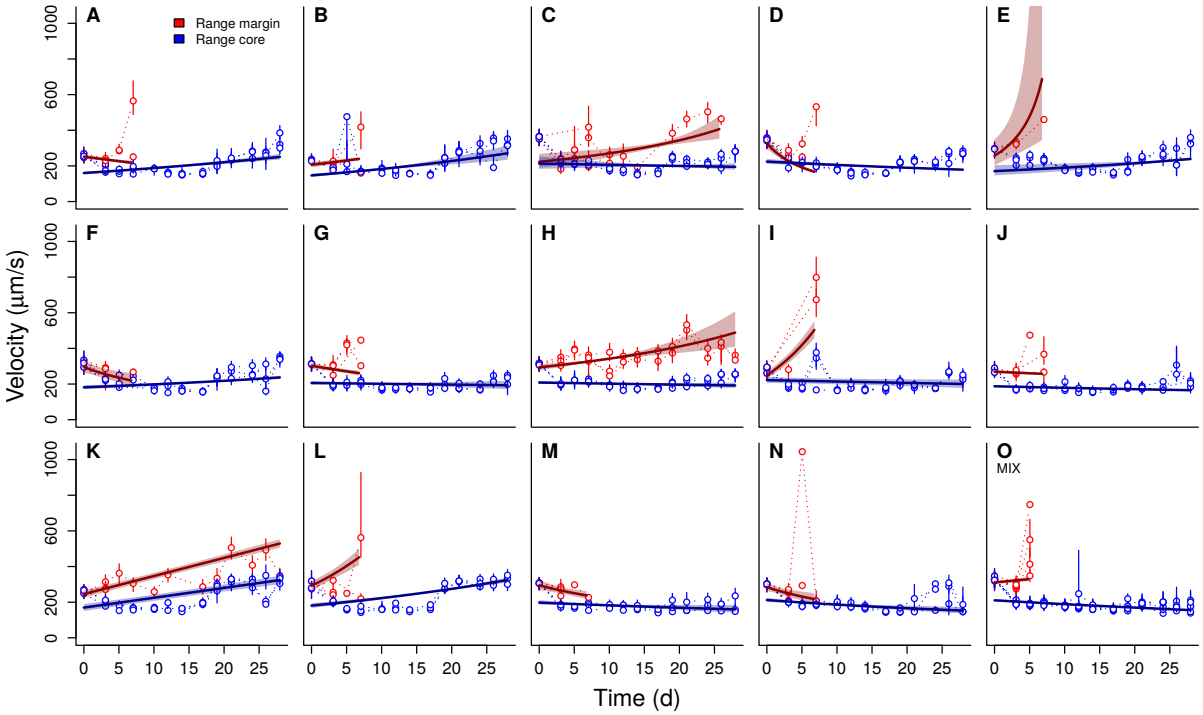

Figure 1: Temporal dynamics of movement velocity during range expansions. While most strains did not expand their range and went extinct, strains C, H and K successfully expanded. Points and error lines show medians and interquartile ranges of the individual-based velocity data for each replicate separately. We additionally show estimates (solid lines) and confidence intervals (shaded area) obtained from the best fitting model correlating velocity and time for range cores (blue) and margins (red; see Supporting Information Tab. S3 for model selection results and sample sizes).

Evolution of movement

All three successfully expanding strains showed increased movement velocity during the experimental evolution phase at the range margin (Tab. S3 and S4). Individuals in populations at the range margin were between 1.14 and 1.7 times faster than individuals in the range core (comparison of estimates; Fig. 2). In one of the strains (Fig. 1 C) these differences could be shown to be stable after a three day common garden (approx. 10 to 20 doubling time periods based on the estimates of r_0 in Tab. S1), thus indicating evolutionary change (Fig. 2 A; difference in velocity between margin and core was reduced to 1.45 fold after the common garden, in comparison to 1.7 fold before). In the other strains (Fig. 1 H and K; Fig. 2 B and C) the difference was therefore likely due to phenotypic plasticity only. After an additional month of strong selection for competitive ability in a common garden setting (common garden 38 days; right panels in Fig. 2) the difference between velocities in range core versus range margin populations was clearly reduced and on average individuals from the range margin were only 1.22 times as fast as

individuals from the range core with strongly overlapping confidence intervals (Fig. 2 A).

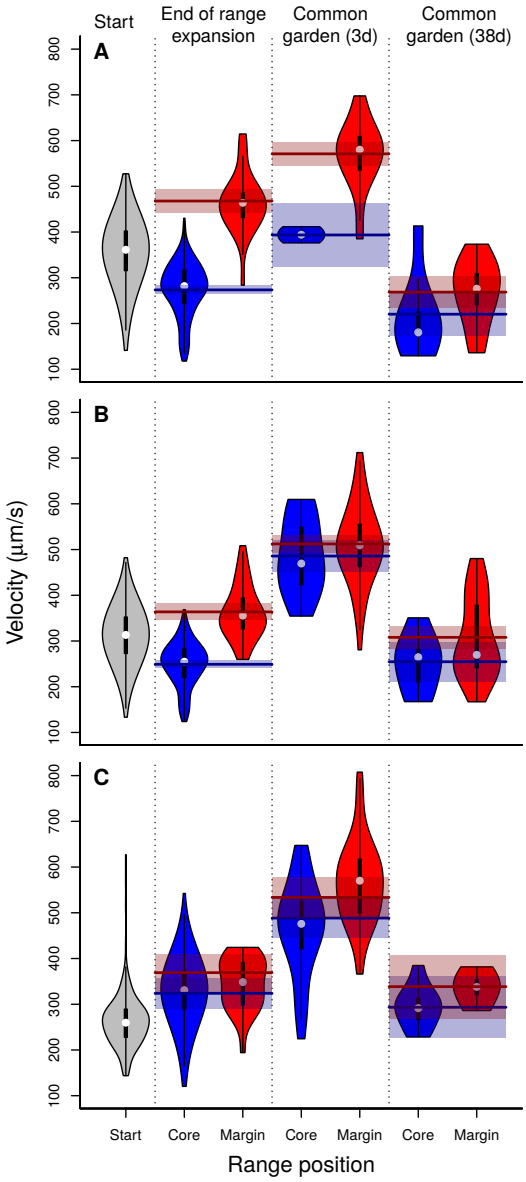

Figure 2: Evolutionary differences in movement velocity between range cores and range margins for the strains that successfully expanded their range (panels A to C, representing strain C, H and K respectively). All strains showed increased movement velocity at the range margin at the end of the range expansion (see also Fig. 1). However, this difference was only stable after the 3-day common garden for strain C (panel A; central column). The violin plots show medians (white dot), the 25th and 75th percentile (box) and the kernel density. We additionally show estimates (solid lines) and confidence intervals (shaded area) obtained from the best fitting model comparing velocity in rage cores and margins at the three represented time points (see Supporting Information Tab. S4 for model selection results and sample sizes). Note that the distribution of velocity at the start of the experiment (grey violin plots) is only shown as a visual reference and not included in the statistical analysis.

While all three strains showed density-dependent movement to some extent (Fig. 3; Tab. S5), only the strain which had shown evolutionary change at the range margin (Fig. 1 C, Fig. 2 A) exhibited clear

differences in density-dependence of movement between range core and range margin populations. The slope of the density-dependent movement reaction norm for range margin populations was clearly reduced and approached a flat line in comparison to the density-dependent movement reaction norm for range core populations which was clearly positively density-dependent (Fig. 3 A; LMM on log-transformed data, estimates and CI; slope(margin): 0.03 (-0.01, 0.08); difference to slope(core): 0.40 (0.25, 0.55); difference to slope(start): 0.01 (-0.04, 0.06); Tab. S5).

Evolution of population growth and competitive ability

Pooling the results from all three strains that successfully tracked the experimental range expansion, we could find clear differences in population growth rates after the common garden phase between range core and range margin (Fig. 4). Range margin populations exhibited population growth rates that were on average 3.2 times higher than range core populations. Conversely, range core populations showed a tendency for increased competitive ability (average increase of 2.2 fold, however with strongly overlapping confidence intervals). Note that these effects were most clear for growth data from strain C (Fig. 4).

Discussion

We investigated emerging evolutionary differentiation between range core and range margin populations using highly controlled and replicated range expansions of both clonal strains without initial standing genetic variation as well as a mix of all strains. The latter not only harboured standing genetic variation but also allowed for sexual reproduction and recombination. Our experimental results give clear evidence of rapidly emerging evolutionary differences in dispersal reaction norms, population growth rate and competitive ability during range expansions (after a total of only 13 dispersal events; Fig. 1).

As expected, de novo evolutionary differentiation occurred only rarely (1 out of 48 replicates), while a purely plastic response was observed slightly more often (in 3 additional replicates; Fig. 2). All other range margin populations went extinct during the temporally advancing range propagation and ultimately failed to expand their range (Fig. 1). It is interesting to note that we did not observe evolutionary change in the replicates that potentially allowed for sexual reproduction and harboured initial standing genetic variation. Most importantly, we could not identify any common attributes of the strains that successfully expanded their range, which substantiates previous findings highlighting the intrinsically stochastic and variable nature of range expansions, both in an ecological (Melbourne and Hastings, 2009; Giometto et al., 2013) and evolutionary context (Ochocki and Miller, 2017; Weiss-Lehman et al., 2017).

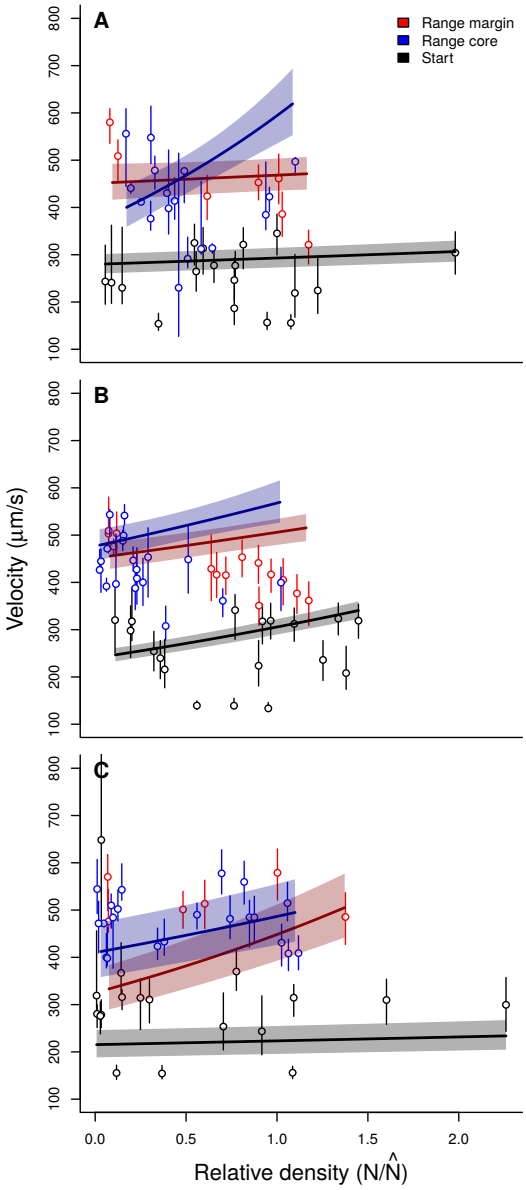

Figure 3: Evolution of density-dependent movement in range cores and at range margins for the strains that successfully expanded their range (panels A to C, representing strain C, H and K respectively). Only strain C (panel A) showed evolutionary differentiation in density-dependent velocity between range core and margin, while no evolutionary difference could be observed for the other two strains H (panel B) and K (panel C). Clearly, the evolutionary difference in velocity between range core and margin reported in Fig. 2 A can be related to increased velocities at low density (panel A). At the same time range core populations of this strain show a pattern of positive density-dependent movement. Points and error lines show medians and interquartile ranges of the individual-based velocity data recorded after the 3-day common garden phase. We additionally show estimates (solid lines) and confidence intervals (shaded area) obtained from the best fitting model of the density-dependent movement reaction norm (see Supporting Information Tab. S5 for model selection results and sample sizes). The x-axis captures the relative density, that is, population size (N) divided by the equilibrium population size ($\hat{N}$) estimated by fitting Eq. 1.

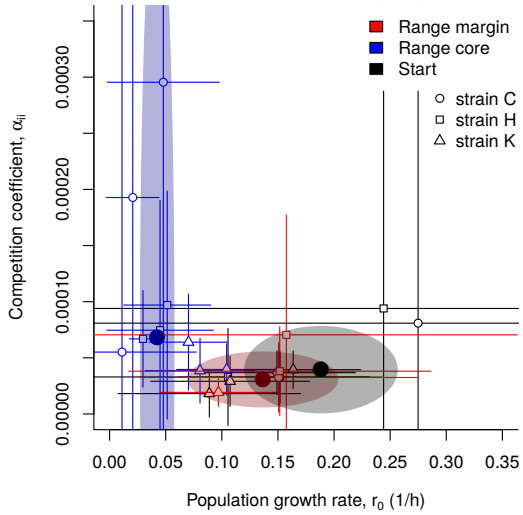

Figure 4: Concurrent evolution of population growth rates (r_0) and competition coefficients (α_{ii}) in range cores and at range margins. Range margin population showed an increased population growth rate in comparison to range cores, which exhibited slightly increased competitive abilities. Points and error lines show estimates and confidence intervals of growth rates (r_0) and competition coefficients (α_{ii}) obtained from fitting the logistic growth model (Eq. 1) to time series data of population growth experiments performed after the 3-day common garden phase. We additionally show estimates (large filled points) and confidence intervals (shaded area) obtained from the best fitting model comparing population growth rate and competition coefficient between range cores, margins and the starting populations (see Supporting Information Tab. S6 for model selection results and sample sizes).

Range expansions can lead to trait evolution even in the absence of initial standing genetic variation.

Selection for increased dispersal at range margins due to spatial selection (Phillips et al., 2010) and potentially kin competition (Kubisch et al., 2013) has been recognized to impact range expansion dynamics theoretically (Kubisch et al., 2014) as well as in comparative and experimental empirical studies (Fronhofer and Altermatt, 2015; Williams et al., 2016; Wagner et al., 2016; Ochocki and Miller, 2017; Weiss-Lehman et al., 2017; Fronhofer et al., in press). However, the relevance of spatial selection for systems that do not initially harbour high amounts of standing genetic variation remained unclear. This is surprising and disturbing, as invasions of non-native organisms, in contrast to expansions of a species' range starting from a large and potentially diverse core habitat, usually start with a colonization event involving one or very few individuals and therefore by default tend to exhibit very little standing genetic variation (e.g., Tsutsui et al. 2000; but see also Roman and Darling 2007). Given the ecological and economical relevance of invasive species (Pimentel et al., 2000), a more coherent understanding of the underlying evolutionary dynamics is critically needed. Our study is set apart from other recent experimental work on range expansions in that the evolutionary differences reported here are not due to selection on standing genetic variation, but emerge de novo during our experiments. We show that differentiation

along a species range in movement and other life-history traits is possible in a relatively short time even without initial standing genetic variation (Figs. 1 and 2).

Besides being applicable to biological invasions our results and conclusions are relevant to climate- or generally environmental change-driven range expansions. Our experimental procedure basically simulates a shifting window of suitable habitat for the range margin as is often done in theoretical studies (e.g. Henry et al., 2013). Fig. 1 highlights that, despite most often leading to extinction, evolutionary change (Fig. 1 C and Fig. 2 A) as well as phenotypic plasticity (Fig. 1 H, K and Fig. 2 B, C) can potentially rescue these marginal populations from extinction (Bell and Gonzalez, 2011; Low-Décarie et al., 2015).

Range expansions select for density-independent movement at range margins.

Importantly, our work shows that dispersal evolution at expanding range margins does not only impact average dispersal probabilities, but changes the shape of the density-dependent dispersal reaction norm (Fig. 3 A). Theory predicts that dispersal should become density-independent at expanding range margins (Travis et al., 2009) because conspecific density looses its value as a cue for context-dependent dispersal. Since potential target patches for range margin populations tend to be empty, dispersal is advantageous already at low densities and an unconditional dispersal strategy will be less costly (Bonte et al., 2012) as energy and time do not have to be invested in information collection and processing.

We find that the starting populations showed weak or no density-dependent movement (Fig. 3). Subsequently, individuals at the range margin conserved this density-independent movement strategy during the range expansion, while individuals in the range core clearly evolved positive density-dependence (Fig. 3 A). Our experimental results therefore substantiate the theoretical predictions of Travis et al. (2009) and are in good accordance with empirical work that suggested a weakening of the slope of density-dependent dispersal function in an insect system (Weiss-Lehman et al., 2017).

Range expansions select for increased reproductive rates at range margins.

While dispersal is a central and potentially independent life-history trait of major importance for spatial dynamics (Bonte and Dahirel, 2017), other life-history traits, such as reproduction may evolve concurrently or even trade-off with dispersal (e.g. Burton et al., 2010; Fronhofer et al., 2011; Stevens et al., 2014; Fronhofer and Altermatt, 2015). Our results show that not only movement capacities but also reproductive rates and competitive abilities may evolve during range expansions and biological invasions (Fig. 4). Substantiating theoretical predictions (e.g. Burton et al., 2010), we experimentally find higher population growth rates at the range margin in comparison to range core populations. Again, it is individuals in the range core that evolved lower growth rates in comparison to individuals at the range margin and in

the starting population and not vice versa. At the same time, we observe higher competitive abilities in range core populations, which hints at a trade-off between competitive ability and population growth rates.

Our results regarding the evolution of population growth and competitive ability, as well as previous findings in a similar system (Fronhofer et al., in press), are opposed to some recent experimental investigations reporting lower reproduction, respectively investment in population growth at the range margin (Fronhofer and Altermatt, 2015; Weiss-Lehman et al., 2017) or no effect on reproduction (Ochocki and Miller, 2017). While this heterogeneity in results may be linked to differences in resource dynamics in the experiments (Fronhofer and Altermatt, 2015; Fronhofer et al., in press), it also hints at the potential evolutionary independence of dispersal from other life-history traits (Bonte and Dahirel, 2017). Clearly, more conceptual and experimental research is needed to provide synthesis on these questions.

Conclusions

We present experimental evidence showing that range expansions lead to the evolution of increased dispersal at range margins and decreased dispersal in range cores due to evolutionary changes in the density-dependent movement reaction norm. Movement evolves to be density-dependent in the range core and density-independent at the range margin. Additionally, we observed concurrent changes in life-history traits towards higher reproduction at the range margin and higher competitive abilities in the range core. Importantly, these evolutionary changes emerge de novo in our experiments and do not require initial standing genetic variation. Our results suggest, that, although rare, evolution can rescue populations from shifting climatic and environmental changes in general by allowing individuals to track their climatic niche by adapted dispersal and growth strategies. At the same time evolution can favour the spread of invasive species, even if standing genetic variation is initially low as in a biological invasion.

Author contributions

E.A.F. and F.A. designed the research; E.A.F. and S.G. performed the experiments; E.A.F. analysed the data and outlined the manuscript; all authors contributed to writing.

Acknowledgements

E.A.F. and F.A. thank Eawag and the Swiss National Science Foundation (grant no. PP00P3_150698 to FA) for funding. We are grateful to Felix Moerman for comments on a previous version of the manuscript.

Literature cited

Altermatt, F., E. A. Fronhofer, A. Garnier, A. Giometto, F. Hammes, J. Klecka, D. Legrand, E. Mächler, T. M. Massie, M. Plebani, F. Pennekamp, M. Pontarp, N. Schtickzelle, V. Thuillier, and O. L. Petchey, 2015. Big answers from small worlds: a user's guide for protist microcosms as a model system in ecology and evolution. Methods Ecol. Evol. 6:218–231. URL `http://onlinelibrary.wiley.com/doi/10.1111/2041-210X.12312/abstract`. The detailed protocols (that appear in the supplement) are available at http://emeh-protocols.readthedocs.org/.

Bell, G. and A. Gonzalez, 2011. Adaptation and evolutionary rescue in metapopulations experiencing environmental deterioration. Science 332:1327–1330.

Best, A. S., K. Johst, T. Munkemuller, and J. M. J. Travis, 2007. Which species will succesfully track climate change? the influence of intraspecific competition and density dependent dispersal on range shifting dynamics. Oikos 116:1531–1539.

Bonte, D. and M. Dahirel, 2017. Dispersal: a central and independent trait in life history. Oikos .

Bonte, D., H. Van Dyck, J. M. Bullock, A. Coulon, M. Delgado, M. Gibbs, V. Lehouck, E. Matthysen, K. Mustin, M. Saastamoinen, N. Schtickzelle, V. M. Stevens, S. Vandewoestijne, M. Baguette, K. Bartoń, T. G. Benton, A. Chaput-Bardy, J. Clobert, C. Dytham, T. Hovestadt, C. M. Meier, S. C. F. Palmer, C. Turlure, and J. M. J. Travis, 2012. Costs of dispersal. Biol. Rev. 87:290–312. URL `http://dx.doi.org/10.1111/j.1469-185X.2011.00201.x`.

Bowler, D. E. and T. G. Benton, 2005. Causes and consequences of animal dispersal strategies: relating individual behaviour to spatial dynamics. Biol. Rev. 80:205–225.

Burton, O. J., B. L. Pillips, and J. M. J. Travis, 2010. Trade-offs and the evolution of life-histories during range expansion. Ecol. Lett. 13:1210–1220.

Cassidy-Hanley, D. M., 2012. Tetrahymena in the laboratory: Strain resources, methods for culture, maintenance, and storage. Methods Cell Biol. 109:237–276. URL http://dx.doi.org/10.1016/B978-0-12-385967-9.00008-6.

Clobert, J., J. F. Le Galliard, J. Cote, S. Meylan, and M. Massot, 2009. Informed dispersal, heterogeneity in animal dispersal syndromes and the dynamics of spatially structured populations. Ecol. Lett. 12:197–209.

Excoffier, L., M. Foll, and R. J. Petit, 2009. Genetic consequences of range expansions. Annu. Rev. Ecol. Evol. Syst. 40:481–501. URL http://dx.doi.org/10.1146/annurev.ecolsys.39.110707.173414.

Fjerdingstad, E., N. Schtickzelle, P. Manhes, A. Gutierrez, and J. Clobert, 2007. Evolution of dispersal and life history strategies — *Tetrahymena* ciliates. BMC Evol. Biol. 7:133. URL http://www.biomedcentral.com/1471-2148/7/133.

Friman, V.-P., J. Laakso, M. Koivu-Orava, and T. Hiltunen, 2011. Pulsed-resource dynamics increase the asymmetry of antagonistic coevolution between a predatory protist and a prey bacterium. J. Evol. Biol. 24:2563–2573. URL http://dx.doi.org/10.1111/j.1420-9101.2011.02379.x.

Fronhofer, E. A. and F. Altermatt, 2015. Eco-evolutionary feedbacks during experimental range expansions. Nat. Commun. 6:6844.

Fronhofer, E. A., J. Klecka, C. Melián, and F. Altermatt, 2015a. Condition-dependent movement and dispersal in experimental metacommunities. Ecol. Lett. 18:954–963. As a preprint on BioRxiv http://dx.doi.org/10.1101/017954.

Fronhofer, E. A., T. Kropf, and F. Altermatt, 2015b. Density-dependent movement and the consequences of the allee effect in the model organism *Tetrahymena*. J. Anim. Ecol. 84:712–722. URL http://onlinelibrary.wiley.com/doi/10.1111/1365-2656.12315/abstract.

Fronhofer, E. A., A. Kubisch, T. Hovestadt, and H. J. Poethke, 2011. Assortative mating counteracts the evolution of dispersal polymorphisms. Evolution 65:2461–2469.

Fronhofer, E. A., N. Nitsche, and F. Altermatt, in press. Information use shapes the dynamics of range expansions into environmental gradients. Glob. Ecol. Biogeogr. As a preprint on BioRxiv http://dx.doi.org/10.1101/056002.

Giometto, A., F. Altermatt, F. Carrara, A. Maritan, and A. Rinaldo, 2013. Scaling body size fluctuations. Proc. Natl. Acad. Sci. U. S. A. 110:4646–4650.

Giometto, A., A. Rinaldo, F. Carrara, and F. Altermatt, 2014. Emerging predictable features of replicated biological invasion fronts. Proc. Natl. Acad. Sci. U. S. A. 111:297–301. URL http://www.pnas.org/content/111/1/297.abstract.

Haag, C. R., M. Saastamoinen, J. H. Marden, and I. Hanski, 2005. A candidate locus for variation in dispersal rate in a butterfly metapopulation. Proc. R. Soc. B-Biol. Sci. 272:2449–2456.

Hanski, I., 2012. Eco-evolutionary dynamics in a changing world. Ann. N. Y. Acad. Sci. 1249:1–17. URL http://dx.doi.org/10.1111/j.1749-6632.2011.06419.x.

Henry, R. C., G. Bocedi, and J. M. Travis, 2013. Eco-evolutionary dynamics of range shifts: Elastic margins and critical thresholds. J. Theor. Biol. 321:1–7. URL http://dx.doi.org/10.1016/j.jtbi.2012.12.004.

Hiltunen, T. and L. Becks, 2014. Consumer co-evolution as an important component of the eco-evolutionary feedback. Nat. Commun. 5:5226. URL http://dx.doi.org/10.1038/ncomms6226.

Kubisch, A., E. A. Fronhofer, H. J. Poethke, and T. Hovestadt, 2013. Kin competition as a major driving force for invasions. Am. Nat. 181:700–706. URL http://www.jstor.org/stable/10.1086/670008.

Kubisch, A., R. D. Holt, H. J. Poethke, and E. A. Fronhofer, 2014. Where am I and why? Synthesising range biology and the eco-evolutionary dynamics of dispersal. Oikos 123:5–22.

Kubisch, A., H. J. Poethke, and T. Hovestadt, 2011. Density-dependent dispersal and the formation of range borders. Ecography 34:1002–1008.

Lombaert, E., A. Estoup, B. Facon, B. Joubard, J.-C. Grgoire, A. Jannin, A. Blin, and T. Guillemaud, 2014. Rapid increase in dispersal during range expansion in the invasive ladybird *Harmonia axyridis*. J. Evol. Biol. 27:508–517. URL http://dx.doi.org/10.1111/jeb.12316.

Low-Décarie, E., M. Kolber, P. Homme, A. Lofano, A. Dumbrell, A. Gonzalez, and G. Bell, 2015. Community rescue in experimental metacommunities. Proc. Natl. Acad. Sci. U. S. A. 112:14307–14312.

Melbourne, B. A. and A. Hastings, 2009. Highly variable spread rates in replicated biological invasions: fundamental limits to predictability. Science 325:1536–1539. URL http://www.sciencemag.org/content/325/5947/1536.short.

Ochocki, B. M. and T. E. X. Miller, 2017. Rapid evolution of dispersal ability makes biological invasions faster and more variable. Nat. Commun. 8:14315.

Pennekamp, F., K. A. Mitchell, A. S. Chaine, and N. Schtickzelle, 2014. Dispersal propensity in *Tetrahymena thermophila* ciliates — a reaction norm perspective. Evolution 68:2319–2330.

Pennekamp, F., N. Schtickzelle, and O. L. Petchey, 2015. Bemovi, software for extracting behavior and morphology from videos, illustrated with analyses of microbes. Ecol. Evol. 5:2584–2595.

Perkins, A. T., B. L. Phillips, M. L. Baskett, and A. Hastings, 2013. Evolution of dispersal and life history interact to drive accelerating spread of an invasive species. Ecol. Lett. 16:1079–1087. URL http://dx.doi.org/10.1111/ele.12136.

Phillips, B. L., G. P. Brown, and R. Shine, 2010. Life-history evolution in range-shifting populations. Ecology 91:1617–1627. URL http://www.esajournals.org/doi/abs/10.1890/09-0910.1.

Phillips, B. L., G. P. Brown, J. K. Webb, and R. Shine, 2006. Invasion and the evolution of speed in toads. Nature 439:803–803. URL http://dx.doi.org/10.1038/439803a.

Pimentel, D., L. Lach, R. Zuniga, and D. Morrison, 2000. Environmental and economic costs of non-indigenous species in the united states. BioScience 50:53–65.

Roman, J. and J. A. Darling, 2007. Paradox lost: genetic diversity and the success of aquatic invasions. Trends Ecol. Evol. 22:454–464.

Ronce, O., 2007. How does it feel to be like a rolling stone? Ten questions about dispersal evolution. Annu. Rev. Ecol. Evol. Syst. 38:231–253.

Stevens, V. M., S. Whitmee, J.-F. Le Galliard, J. Clobert, K. Böhning-Gaese, D. Bonte, M. Brändle, D. Matthias Dehling, C. Hof, A. Trochet, and M. Baguette, 2014. A comparative analysis of dispersal syndromes in terrestrial and semi-terrestrial animals. Ecol. Lett. 17:1039–1052. URL http://dx.doi.org/10.1111/ele.12303.

Thomas, C. D., E. J. Bodsworth, R. J. Wilson, A. D. Simmons, Z. G. Davies, M. Musche, and L. Conradt, 2001. Ecological and evolutionary processes at expanding range margins. Nature 411:577–581. URL http://dx.doi.org/10.1038/35079066.

Travis, J. M. J., K. Mustin, T. G. Benton, and C. Dytham, 2009. Accelerating invasion rates result from the evolution of density-dependent dispersal. J. Theor. Biol. 259:151–158.

Tsutsui, N. D., A. V. Suarez, D. A. Holway, and T. J. Case, 2000. Reduced genetic variation and the success of an invasive species. Proc. Natl. Acad. Sci. U. S. A. 97:5948–5953.

Verhulst, P.-F., 1838. Notice sur la loi que la population suit dans son accroissement. Correspondance Mathématique et Physique 10:113–121.

Wagner, N. K., B. M. Ochocki, K. M. Crawford, A. Compagnoni, and T. E. Miller, 2016. Genetic mixture of multiple source populations accelerates invasive range expansion. J. Anim. Ecol. URL http://dx.doi.org/10.1111/1365-2656.12567.

Weiss-Lehman, C., R. A. Hufbauer, and B. A. Melbourne, 2017. Rapid trait evolution drives increased speed and variance in experimental range expansions. Nat. Commun. 8:14303.

Williams, J. L., B. E. Kendall, and J. M. Levine, 2016. Rapid evolution accelerates plant population spread in fragmented experimental landscapes. Science 353:482–485. URL http://dx.doi.org/10.1126/science.aaf6268.

Supporting Information

E.A. Fronhofer, S. Gut and F. Altermatt:

Evolution of density-dependent movement during replicated experimental range expansions

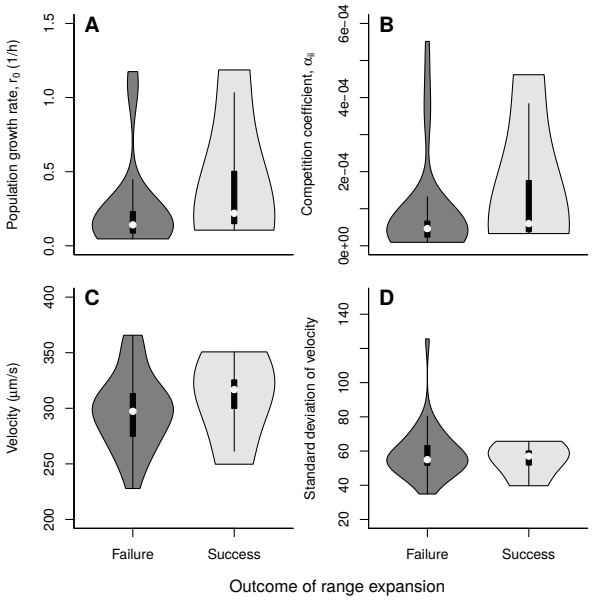

Figure S1: Differences between successful and failed range expansions. The statistical analysis (see Tab. S7) did not detect any differences in strain properties at the start of the experiment between failed an successful range expansions. The violin plots show medians (white dot), the 25th and 75th percentile (box) and the kernel density.

Table S1: Strain characteristics: population dynamics. We report median and quartiles of 3 replicates.

Strain ID	**Mating type**	**Isolate**	**Population growth rate** r_0 (h^{-1})	**Competition coefficient** α_{ii} (1E-05 h^{-1})	**Equilibrium density** $\hat{N}$ (mL^{-1})
A	I	A	0.26 (0.17, 0.27)	6.47 (4.34, 8.38)	3958 (3327, 4046)
B	I	B	0.16 (0.12, 0.18)	5.71 (4.16, 6.96)	2881 (2580, 2895)
C	II	A	0.15 (0.15, 0.21)	3.68 (3.48, 5.88)	4055 (3727, 4346)
D	II	B	0.22 (0.18, 0.23)	5.38 (4.41, 5.90)	3971 (3902, 3989)
E	III	A	0.06 (0.05, 0.07)	1.99 (1.88, 2.67)	2625 (2306, 2850)
F	III	B	0.16 (0.14, 0.62)	7.27 (6.30, 26.47)	2180 (2138, 2272)
G	IV	A	0.21 (0.16, 0.64)	5.37 (5.29, 20.09)	3079 (2626, 3533)
H	IV	B	0.24 (0.17, 0.72)	9.40 (6.35, 27.78)	2598 (2584, 2900)
I	V	A	0.15 (0.11, 0.61)	5.76 (3.82, 20.84)	2962 (2754, 3219)
J	V	B	0.21 (0.13, 0.69)	9.60 (6.19, 32.38)	2131 (1993, 2167)
K	VI	A	0.11 (0.10, 0.14)	2.91 (2.36, 3.42)	4152 (3921, 4525)
L	VI	B	0.06 (0.06, 0.07)	0.97 (0.95, 1.07)	6259 (6126, 6425)
M	VII	A	0.13 (0.12, 0.20)	2.67 (2.52, 4.05)	4743 (4642, 4975)
N	VII	B	0.13 (0.10, 0.18)	4.10 (2.75, 5.29)	3480 (3381, 4141)

Table S2: Strain characteristics: morphology and Movement. We report median and quartiles of 3 replicates.

Strain ID	Mating type	Isolate	Size (μm)	Aspect ratio	Velocity ($\mu m s^{-1}$)	Sd. turning angle	Net velocity ($\mu m s^{-1}$)
A	I	A	54.58 (51.25, 58.26)	1.44 (1.35, 1.57)	258 (228, 290)	0.32 (0.25, 0.40)	5.62 (3.22, 8.39)
B	I	B	55.07 (51.17, 59.70)	1.31 (1.28, 1.37)	231 (208, 264)	0.30 (0.21, 0.37)	4.56 (2.74, 7.92)
C	II	A	57.58 (53.94, 60.65)	1.38 (1.34, 1.43)	361 (316, 402)	0.36 (0.30, 0.43)	6.32 (3.64, 9.92)
D	II	B	55.84 (52.11, 59.03)	1.39 (1.34, 1.45)	347 (300, 391)	0.38 (0.30, 0.46)	6.43 (3.74, 10.23)
E	III	A	64.36 (58.76, 68.48)	1.30 (1.26, 1.37)	296 (259, 332)	0.28 (0.23, 0.36)	6.32 (3.40, 9.38)
F	III	B	62.39 (58.23, 66.20)	1.32 (1.28, 1.38)	306 (262, 352)	0.27 (0.20, 0.34)	6.30 (3.29, 10.03)
G	IV	A	57.87 (53.47, 61.45)	1.38 (1.33, 1.45)	313 (274, 351)	0.35 (0.27, 0.42)	5.72 (3.47, 9.15)
H	IV	B	58.05 (54.14, 61.64)	1.39 (1.33, 1.45)	313 (273, 352)	0.33 (0.25, 0.40)	6.36 (3.84, 9.98)
I	V	A	63.78 (58.95, 67.95)	1.34 (1.29, 1.41)	276 (235, 312)	0.35 (0.26, 0.42)	5.24 (3.10, 8.66)
J	V	B	62.89 (58.88, 66.74)	1.34 (1.29, 1.40)	281 (243, 313)	0.33 (0.25, 0.40)	5.46 (3.24, 8.73)
K	VI	A	59.13 (55.56, 63.20)	1.31 (1.27, 1.38)	260 (228, 289)	0.35 (0.28, 0.43)	4.40 (2.60, 6.99)
L	VI	B	60.59 (55.67, 64.80)	1.32 (1.27, 1.40)	288 (257, 329)	0.34 (0.27, 0.42)	4.25 (2.43, 7.29)
M	VII	A	64.38 (59.96, 69.24)	1.37 (1.32, 1.43)	306 (271, 337)	0.34 (0.27, 0.41)	5.72 (3.31, 8.81)
N	VII	B	63.02 (58.15, 67.01)	1.37 (1.32, 1.45)	301 (265, 335)	0.37 (0.31, 0.44)	5.22 (3.07, 8.33)

Table S3: Model selection: temporal dynamics of movement during range expansions. We report model structure, including possible transformations, as well as differences in AICc values relative to the best model (smallest AICc), AICc weights and sample sizes. The sample size captures the total number of individual data points used and the value in brackets indicates the number of experimental replicates. Bold font indicates the selected model. A visualization of the best fitting model (estimates and confidence intervals) can be found in Fig. 1. In all cases the random effect structure was 'time' nested in 'replicate'.

Figure	Model	ΔAICc	W_{AICc}	N
1 A	$log(velocity) \sim 1$	2598.66	0	
1 A	$log(velocity) \sim position$	75.35	0	
1 A	$log(velocity) \sim time$	2589.82	0	
1 A	$log(velocity) \sim time + position$	64.70	0	
1 A	$\mathbf{log(velocity) \sim time \cdot position}$	**0**	**1**	**12392 (3)**
1 B	$log(velocity) \sim 1$	287.13	0	
1 B	$log(velocity) \sim position$	11.36	0	
1 B	$log(velocity) \sim time$	280.91	0	
1 B	$\mathbf{log(velocity) \sim time + position}$	**0**	**0.58**	**7486 (3)**
1 B	$log(velocity) \sim time \cdot position$	0.65	0.42	
1 C	$velocity^{-1} \sim 1$	4482.42	0	
1 C	$velocity^{-1} \sim position$	1358.54	0	
1 C	$velocity^{-1} \sim time$	4484.42	0	
1 C	$velocity^{-1} \sim time + position$	1360.49	0	
1 C	$\mathbf{velocity^{-1} \sim time \cdot position}$	**0**	**1**	**30199 (3)**
1 D	$velocity^{-1} \sim 1$	1003.83	0	
1 D	$velocity^{-1} \sim position$	470.25	0	
1 D	$velocity^{-1} \sim time$	985.94	0	
1 D	$velocity^{-1} \sim time + position$	458.57	0	
1 D	$\mathbf{velocity^{-1} \sim time \cdot position}$	**0**	**1**	**16192 (3)**
1 E	$velocity^{-1} \sim 1$	194.18	0	
1 E	$velocity^{-1} \sim position$	9.56	0.01	
1 E	$velocity^{-1} \sim time$	191.62	0	
1 E	$velocity^{-1} \sim time + position$	6.11	0.04	
1 E	$\mathbf{velocity^{-1} \sim time \cdot position}$	**0**	**0.95**	**9109 (3)**
1 F	$velocity^{-1} \sim 1$	310.84	0	
1 F	$velocity^{-1} \sim position$	18.74	0	
1 F	$velocity^{-1} \sim time$	303.03	0	
1 F	$velocity^{-1} \sim time + position$	11.24	0	
1 F	$\mathbf{velocity^{-1} \sim time \cdot position}$	**0**	**1**	**9099 (3)**
1 G	$log(velocity) \sim 1$	1786.13	0	
1 G	$log(velocity) \sim position$	14.23	0	
1 G	$log(velocity) \sim time$	1785.97	0	
1 G	$log(velocity) \sim time + position$	15.45	0	
1 G	$\mathbf{log(velocity) \sim time \cdot position}$	**0**	**1**	**15042 (3)**
1 H	$velocity^{-1} \sim 1$	18493.41	0	
1 H	$velocity^{-1} \sim position$	1259.41	0	
1 H	$velocity^{-1} \sim time$	18492.38	0	
1 H	$velocity^{-1} \sim time + position$	1257.66	0	
1 H	$\mathbf{velocity^{-1} \sim time \cdot position}$	**0**	**1**	**26903 (3)**
1 I	$log(velocity) \sim 1$	671.58	0	
1 I	$log(velocity) \sim position$	328.30	0	
1 I	$log(velocity) \sim time$	670.00	0	
1 I	$log(velocity) \sim time + position$	328.56	0	
1 I	$\mathbf{log(velocity) \sim time \cdot position}$	**0**	**1**	**8616 (3)**

Table continued on the next page.

Figure	Model	ΔAICc	W_{AICc}	N
1 J	$velocity^{-1} \sim 1$	955.41	0	
1 J	$velocity^{-1} \sim position$	6.60	0.02	
1 J	$velocity^{-1} \sim time$	940.33	0	
1 J	$\mathbf{velocity^{-1} \sim time + position}$	**0**	**0.65**	**5520 (3)**
1 J	$velocity^{-1} \sim time \cdot position$	1.36	0.33	
1 K	$velocity \sim 1$	5664.26	0	
1 K	$velocity \sim position$	397.60	0	
1 K	$velocity \sim time$	5655.46	0	
1 K	$velocity \sim time + position$	382.16	0	
1 K	$\mathbf{velocity \sim time \cdot position}$	**0**	**1**	**16641 (3)**
1 L	$log(velocity) \sim 1$	692.68	0	
1 L	$log(velocity) \sim position$	51.88	0	
1 L	$log(velocity) \sim time$	669.88	0	
1 L	$log(velocity) \sim time + position$	27.80	0	
1 L	$\mathbf{log(velocity) \sim time \cdot position}$	**0**	**1**	**9996 (3)**
1 M	$velocity^{-1} \sim 1$	922.79	0	
1 M	$velocity^{-1} \sim position$	5.35	0.06	
1 M	$velocity^{-1} \sim time$	919.58	0	
1 M	$velocity^{-1} \sim time + position$	3.78	0.12	
1 M	$\mathbf{velocity^{-1} \sim time \cdot position}$	**0**	**0.82**	**8246 (3)**
1 N	$velocity^{-1} \sim 1$	716.12	0	
1 N	$velocity^{-1} \sim position$	6.08	0.03	
1 N	$velocity^{-1} \sim time$	711.24	0	
1 N	$velocity^{-1} \sim time + position$	2.10	0.25	
1 N	$\mathbf{velocity^{-1} \sim time \cdot position}$	**0**	**0.72**	**17008 (3)**
1 O	$log(velocity) \sim 1$	2784.45	0	
1 O	$log(velocity) \sim position$	49.01	0	
1 O	$log(velocity) \sim time$	2760.54	0	
1 O	$log(velocity) \sim time + position$	25.33	0	
1 O	$\mathbf{log(velocity) \sim time \cdot position}$	**0**	**1**	**20528 (6)**

Table S4: Model selection: evolutionary differences in movement between range cores and range margins. We report model structure, including possible transformations, as well as differences in AICc values relative to the best model (smallest AICc), AICc weights and sample sizes. The sample size captures the total number of individual data points used and the value in brackets indicates the number of experimental replicates. Bold font indicates the selected model. A visualization of the best fitting model (estimates and confidence intervals) can be found in Fig. 2. In all cases the random effect structure was 'time' nested in 'replicate'.

Figure	**Model**	**ΔAICc**	W_{AICc}	**N**
2 A	$velocity \sim 1$	215.74	0	
2 A	$velocity \sim position$	44.08	0	
2 A	$velocity \sim time$	204.19	0	
2 A	$velocity \sim time + position$	16.98	0	
2 A	$\mathbf{velocity \sim time \cdot position}$	**0**	**1**	**543 (3)**
2 B	$velocity \sim 1$	159.02	0	
2 B	$velocity \sim position$	30.20	0	
2 B	$velocity \sim time$	128.52	0	
2 B	$velocity \sim time + position$	15.16	0	
2 B	$\mathbf{velocity \sim time \cdot position}$	**0**	**1**	**472 (3)**
2 C	$velocity \sim 1$	23.60	0	
2 C	$velocity \sim position$	13.13	0	
2 C	$velocity \sim time$	13.82	0	
2 C	$\mathbf{velocity \sim time + position}$	**0**	**0.83**	**1425 (3)**
2 C	$velocity \sim time \cdot position$	3.20	0.17	

Table S5: Model selection: evolution of density-dependent movement in range cores and at range margins. We report model structure, including possible transformations, as well as differences in AICc values relative to the best model (smallest AICc), AICc weights and sample sizes. The sample size captures the total number of individual data points used and the value in brackets indicates the number of experimental replicates. Bold font indicates the selected model. A visualization of the best fitting model (estimates and confidence intervals) can be found in Fig. 3. In all cases the random effect structure was 'time' nested in 'replicate'.

Figure	**Model**	**ΔAICc**	W_{AICc}	**N**
3 A	$log(velocity) \sim 1$	3516.96	0	
3 A	$log(velocity) \sim history$	64.75	0	
3 A	$log(velocity) \sim density$	3353.47	0	
3 A	$log(velocity) \sim density + history$	24.68	0	
3 A	$\mathbf{log(velocity) \sim density \cdot history}$	**0**	**1**	**10644 (3)**
3 B	$log(velocity) \sim 1$	5624.48	0	
3 B	$log(velocity) \sim historysition$	390.20	0	
3 B	$log(velocity) \sim density$	5567.50	0	
3 B	$log(velocity) \sim density + history$	31.27	0	
3 B	$\mathbf{log(velocity) \sim density \cdot history}$	**0**	**1**	**8610 (3)**
3 C	$velocity^{-1} \sim 1$	7124.00	0	
3 C	$velocity^{-1} \sim history$	197.43	0	
3 C	$velocity^{-1} \sim density$	6972.58	0	
3 C	$velocity^{-1} \sim density + history$	166.35	0	
3 C	$\mathbf{velocity^{-1} \sim density \cdot history}$	**0**	**1**	**10368 (3)**

Table S6: Model selection: concurrent evolution of population growth and competitive ability in range cores and at range margins. We report model structure, including possible transformations, as well as differences in AICc values relative to the best model (smallest AICc), AICc weights and sample sizes. The sample size captures the number of growth experiments used to estimate r_0 and α_{ii}. Bold font indicates the selected model. A visualization of the best fitting model (estimates and confidence intervals) can be found in Fig. 4. In all cases 'strain ID' was included as a random effect.

Figure	**Model**	**ΔAICc**	W_{AICc}	**N**
4	$log(r_0) \sim 1$	10.6	0	
4	$\mathbf{log(r_0) \sim history}$	**0**	**1**	**22**
4	$\alpha^{-1} \sim 1$	2.43	0.23	
4	$\mathbf{\alpha^{-1} \sim history}$	**0**	**0.77**	**22**

Table S7: Model selection: differences between successful and failed range expansions. .We report model structure, including possible transformations, as well as differences in AICc values relative to the best model (smallest AICc), AICc weights and sample sizes. The sample size captures the total number of replicates. Bold font indicates the selected model. See also Fig. S1. In all cases 'strain ID' was included as a random effect.

Figure	**Model**	**ΔAICc**	W_{AICc}	**N**
S1 A	$\mathbf{r_0^{-1} \sim 1}$	**0**	**0.65**	**40**
S1 A	$r_0^{-1} \sim success$	1.25	0.35	
S1 B	$\mathbf{\alpha^{-1} \sim 1}$	**0**	**0.66**	**40**
S1 B	$\alpha^{-1} \sim success$	1.33	0.34	
S1 C	$\mathbf{log(median\ velocity) \sim 1}$	**0**	**0.72**	**40**
S1 C	$log(median\ velocity) \sim success$	1.92	0.28	
S1 D	$\mathbf{(sd\ velocity)^{-1} \sim 1}$	**0**	**0.53**	**40**
S1 D	$(sd\ velocity)^{-1} \sim success$	0.23	0.47	